Density-functional calculations of the crystal structures and properties of $CsCr_3O_8$ and ACr_3O_8 (A=In,Tl,Cu,Ag,Au)

R. Vidya,* P. Ravindran, A. Kjekshus, and H. Fjellvåg
Department of Chemistry, University of Oslo, Box 1033 Blindern, N-0315 Oslo, Norway
(Received 26 October 2005; revised manuscript received 23 March 2006; published 1 May 2006)

Accurate *ab initio* density-functional calculations are performed to predict ground-state crystal structures and to gain understanding of electronic structure and magnetic properties of $CsCr_3O_8$ and ACr_3O_8 (A=In,Tl,Cu,Ag,Au). $CsCr_3O_8$ stabilizes in an orthorhombic (prototype; *Pnma*) structure in agreement with experimental findings whereas the remaining compounds stabilize in the monoclinic KCr_3O_8-type ($C2/m$) structure. All compounds exhibit antiferromagnetic ordering in the ground state at 0 K. The electronic structures are analyzed with the help of density-of-states, charge-density, and electron-localization-function plots. All compounds (except $InCr_3O_8$) are found to be semiconductors (insulators at 0 K) with very small band gaps, and Cr atoms in different environments consistently take different valence states.

DOI: 10.1103/PhysRevB.73.184101 PACS number(s): 71.20.−b, 78.20.Ci

I. INTRODUCTION

Oxide materials with transition metal constituents in mixed-valence states have attracted much attention in recent years since they exhibit exotic phenomena like colossal magnetoresistance (CMR) and spin, charge, and orbital ordering.[1] Transition-metal compounds with mixed-valence Mn, Cu, and Co are widely studied, whereas others with say, Cr and Ni are less explored. Even though manganates have been attracting much attention for mixed-valence behavior and charge ordering features, mixed-valence states like V^{4+} and V^{5+} in α-NaV_2O_5,[2,3] Ti^{3+}, Ti^{4+} in Ti_4O_7,[4] Ni^{2+} and Ni^{4+} in $HoNiO_3$ (Ref. 5) have also been reported. However, compounds with Cr atoms in mixed-valence states are seldom observed.

In an effort to gain understanding of mixed-valence Cr compounds, we have earlier[6–8] studied structural stability, electronic structure, and magnetic properties for compounds with the general formula ACr_3O_8 (A=H,Li,Na,K,Rb as well as A absent) where Cr formally takes two different valence states. In the first report[6] we used accurate density-functional theory (DFT) calculations to analyze electronic, magnetic, and bonding characteristics of ACr_3O_8 (Na, K, Rb) and later[7] we explored the ground-state structures of Cr_3O_8 and $LiCr_3O_8$ which are of considerable interest as cathode materials in rechargeable Li-ion batteries. In Ref. 8 we report the findings for the highly hypothetical compound HCr_3O_8. In the present work we analyze the structural behavior, electronic structure, and magnetic properties of the corresponding ACr_3O_8 phases with A=Cs, In, Tl, Cu, Ag, and Au, with some special emphasis on $CsCr_3O_8$. One of the salient features of these compounds is that in addition to mixed-valence states, they have layered structures. Among the layered materials with CMR behavior, manganites like $La_{2-2x}Sr_{1+2x}Mn_2O_7$ have been receiving attention recently as they have strong anisotropy of electrical and magnetic transport, anomalous magnetoelastic properties, etc.[9] Therefore the studied compounds may also exhibit interesting physical properties.

II. COMPUTATIONAL DETAILS

The results presented here are based on density-functional calculations according to the projected-augmented plane-wave (PAW) (Ref. 10) method as implemented in the VASP (Vienna *ab initio* simulation package).[11] In this approach the valence orbitals are expanded as plane waves and the interactions between the core and valence electrons are described by pseudopotentials. Since one of the main aims of the present work is to determine ground-state structures for ACr_3O_8, we have performed structural optimizations. We considered around 12 different structure types as inputs for each compound and evaluated the total energy for these test structures. A detailed listing of all the considered input structures are given elsewhere.[6,7] The optimization of the atomic geometry is performed via a conjugate-gradient minimization of the total energy, using Hellmann-Feynman forces on the atoms and stresses in the unit cell. During the simulations, atomic coordinates and axial ratios are allowed to relax for different volumes of the unit cell. These parameters are changed iteratively so that the sum of lattice energy and electronic free energy converges to a minimum value. Convergence minimum with respect to atomic shifts is assumed to have been attained when the energy difference between two successive iterations is less than 10^{-7} eV per cell and the forces acting on the atoms are less than 1 meV $Å^{-1}$. The structure with the lowest total energy is taken as the ground-state structure. The generalized gradient approximation (GGA) includes the effects of local gradients of the charge density and generally gives better equilibrium structural parameters than the local density approximation (LDA). Hence we have used GGA with the Perdew-Burke-Ernzerhof [PBE (Ref. 12)] functional to obtain the accurate exchange and correlation energy for a particular atomic configuration. We have used 520 eV plane-wave energy cutoff for all the compounds. The calculations are carried out using 64 **k** points in the irreducible Brillouin zone for the monoclinic $C2/m$ structure. We have used same energy cutoff and **k**-point density in all calculations. The above calculations are performed in paramagnetic (P), ferromagnetic (F), and antiferromag-

netic (AF) configurations. We have assumed a simple AF structure as shown in Fig. 1(b) of Ref. 6. The magnetic moments are estimated inside the atomic sphere radii. We have calculated the total energy of the compounds as a function of volume for 10 different volumes, fitted the results to the so-called "universal equation of state,"[13] and extracted the bulk modulus (B_0).

III. RESULTS AND DISCUSSION

A. Structural optimization

Among the different atomic arrangements used as inputs in the calculations for $CsCr_3O_8$, the experimentally established[14] structure (prototype; *Pnma*) and the KCr_3O_8-type ($C2/m$) variant came out with lower energies [Fig. 2(a)] than the other considered alternatives. Among these the experimental arrangement has the lowest energy and represents the ground state. The structure [Fig. 1(a)] comprises three crystallographic types of Cr and six types of O atoms which form $Cr1O_6$ octahedra, $Cr2O_4$ tetrahedra, and $Cr3O_4$ tetrahedra. These polyhedra are linked by corner sharing to form layers extending parallel to the *bc* plane, separated by Cs atoms which occupy interlayer positions. The calculated lattice parameters and atom positions for $CsCr_3O_8$ are found to be in reasonable agreement with the available experimental values,[14] except that *a* shows nearly 5.5% deviation between theory and experiment (see Table I). Note that the $CsCr_3O_8$ structure arranges the Cr–O polyhedral layers along the *a* direction. It is in this direction one also finds the interlayer interactions that are governed by the weaker van der Waals type forces, which are not accounted properly by the DFT calculations. This may be the reason for overestimation of *a* and consequently for the somewhat too large equilibrium volume (remembering that GGA alone[15] is likely to overestimate volume by 2%–3%).

Among the considered structures for $CuCr_3O_8$, our structural optimization shows that KCr_3O_8-type ($C2/m$), $LiCr_3O_8$-II-type, and ZnV_3O_8-type ($Iba2$) structures are present at the lower energy region in the total energy vs volume curve. On the other hand, the other ACr_3O_8 compounds under consideration ($A=$In, Tl, Ag, Au) have lower energies for KCr_3O_8-type, $LiCr_3O_8$-type, and LiV_3O_8-type ($P2_1/m$) structures [see Figs. 2(b) and 2(c); for the sake of clarity higher-energy structures are left out]. Hence the ACr_3O_8 compounds with $A=$In, Tl, Cu, Ag, and Au stabilize in the KCr_3O_8-type structure like the alkali-metal derivatives of the family.[6–8,16] The KCr_3O_8-type structure [Fig. 1(b)] consists of two types of Cr atoms arranged in fairly regular octahedral and tetrahedral environments of O neighbors. These polyhedra form layers parallel to the a,b plane by corner sharing and the *A* atoms in interlayer positions. The atomic arrangement in $CsCr_3O_8$ (*Pnma*) is similar to that in the KCr_3O_8-type structure, except that the orientation of half of the tetrahedra of the former is different, and every second layer is rotated by 180° compared with the layers in the KCr_3O_8-type structure. There is a significant distinction between the Cr-O distances in CrO_6 octahedra and CrO_4 tetrahedra in these structures, which immediately points to a mixed-valence situation for Cr.

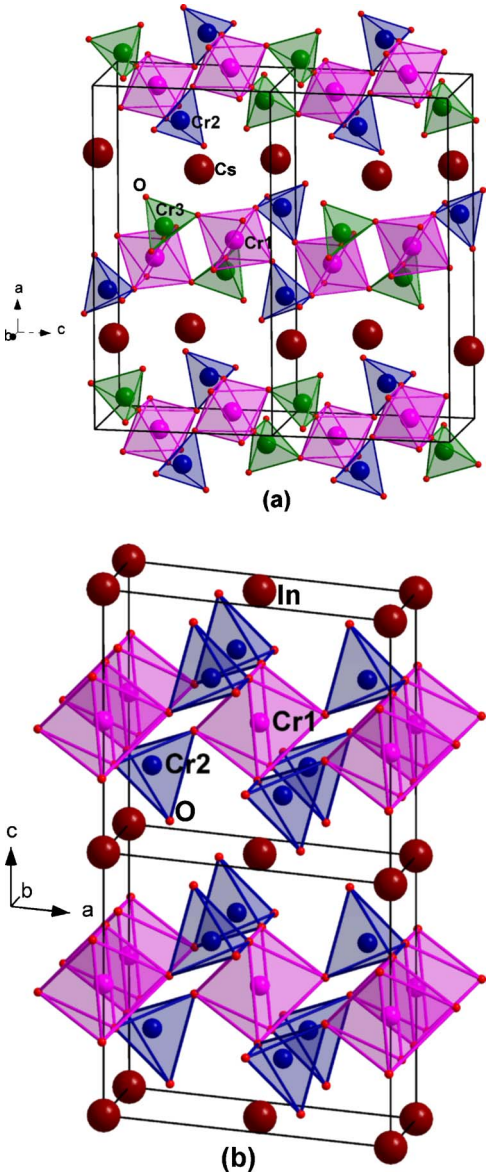

FIG. 1. (Color online) The optimized crystal structures of (a) $CsCr_3O_8$ (prototype; *Pnma*) and (b) $InCr_3O_8$ (KCr_3O_8 type; $C2/m$).

Optimized structural parameters for the ground state of the ACr_3O_8 compounds are given in Table I. Except for a rough linear relationship between the cell volume and the ionic radius of *A* (Fig. 3) there appears to be no clear cut overall trend in the structural parameters for the ACr_3O_8 series as a whole (despite the fact that all members except $CsCr_3O_8$ are formally isostructural). Among the ACr_3O_8 compounds with $A=$In, Tl, Cu, Ag, and Au, only $AgCr_3O_8$ and $TlCr_3O_8$ has been synthesized and characterized by magnetic measurements (but structural determination has not been attempted). Thus, the compounds with $A=$In, Cu, and Au hitherto remain hypothetical. However, the negative values of heat of formation indicate that these materials can be synthesized experimentally.

B. Magnetic properties

Cooperative magnetism with P, F, and AF configurations was taken into account in the structural optimization calcu-

TABLE I. Optimized ground-state structural parameters, bulk modulus (B_0), and heat of formation ($-\Delta H$) for ACr_3O_8 (A=Cs, In, Tl, Cu, Ag, and Au) at 0 K. Except $CsCr_3O_8$ (space group *Pnma*) these compounds stabilize in KCr_3O_8-type structure; space group $C2/m$ with A in 2*a* (0 0 0) and Cr1 in 2*c* (0 0 1/2) positions.

Compound	Unit cell (Å or °)	Positional parameters	B_0 (GPa)	$-\Delta H$ (kJ Mol^{-1})
$CsCr_3O_8$	a=16.8322 (15.9570)[a]	Cs (4*c*): 0.2301, 1/4, 0.0150 (0.2137,1/4,0.0064)	18.96	2189.38
	b=5.5226 (5.5050)	Cr1 (4*c*): 0.4608, 1/4, 0.2575 (0.4524,1/4,0.2407)		
	c=8.5903 (8.264)	Cr2 (4*c*): 0.6046, 1/4, 0.9516 (0.6104,1/4,0.9581)		
		Cr3 (4*c*): 0.9198, 1/4, 0.8714 (0.9205,1/4,0.8627)		
		O1 (4*c*): 0.8340, 1/4, 0.7831 (0.8370,1/4,0.7619)		
		O2 (4*c*): 0.1799, 1/4, 0.4294 (0.1822,1/4,0.4101)		
		O3 (4*c*): 0.0185, 1/4, 0.4515 (0.0110,1/4,0.4699)		
		O4 (4*c*): 0.3996, 1/4, 0.4345 (0.3842,1/4,0.4459)		
		O5 (8*d*): 0.3884, 0.9979, 0.1619 (0.3766, 0.9887, 0.1570)		
		O6 (8*d*): 0.0294, 0.0006, 0.1759 (0.0242, 0.0009, 0.1743)		
$InCr_3O_8$	a=8.4711	Cr2 (4*i*): 0.3576, 0, 0.2641	83.32	2005.53
	b=5.6404	O1 (4*i*): 0.7771, 0, 0.5478		
	c=6.5323	O2 (4*i*): 0.7428, 0, 0.9571		
	β=90.04	O3 (8*j*): 0.9721, 0.7614, 0.2741		
$TlCr_3O_8$	a=8.9606	Cr2 (4*i*): 0.3604, 0, 0.2942	27.91	2543.62
	b=5.5066	O1 (4*i*): 0.7918, 0, 0.5729		
	c=7.7331	O2 (4*i*): 0.6834, 0, 0.9082		
	β=92.84	O3 (8*j*): 0.9630, 0.7541, 0.3271		
$CuCr_3O_8$	a=8.3412	Cr2 (4*i*): 0.3462, 0, 0.2707	20.17	1862.75
	b=5.5182	O1 (4*i*): 0.7727, 0, 0.5360		
	c=6.5480	O2 (4*i*): 0.7708, 0, 0.9434		
	β=94.32	O3 (8*j*): 0.9631, 0.7577, 0.2797		
$AgCr_3O_8$	a=8.6410	Cr2 (4*i*): 0.3444, 0, 0.2848	23.34	1829.89
	b=5.5211	O1 (4*i*): 0.7840, 0, 0.5525		
	c=7.1954	O2 (4*i*): 0.7473, 0, 0.9219		
	β=93.80	O3 (8*j*): 0.9566, 0.7553, 0.3064		
$AuCr_3O_8$	a=8.7686	Cr2 (4*i*): 0.3412, 0, 0.2796	68.04	1706.14
	b=5.4699	O1 (4*i*): 0.7860, 0, 0.5484		
	c=7.0013	O2 (4*i*): 0.7577, 0, 0.9254		
	β=91.50	O2 (8*j*): 0.9543, 0.7551, 0.3006		

[a]Experimental value from Ref. 14.

lations. As seen from Fig. 2 all the studied compounds stabilize in the AF state. According to the measured[17] magnetic susceptibility data, $AgCr_3O_8$ orders antiferromagnetically at low temperatures; magnetic moment derived from the Curie-Weiss relationship gives $\mu_P = 3.95 \pm 0.03 \mu_B$ f.u.$^{-1}$ Calculated magnetic moments for the studied compounds in their ground-state structures are listed in Table II. It is evident that the octahedral Cr1 site carries an appreciable magnetic moment whereas the tetrahedral Cr2 site (as well as Cr3 for $CsCr_3O_8$) has an almost negligible magnetic moment (more significant but still small at the Cr2 and Cr3 sites in $CsCr_3O_8$).

$InCr_3O_8$ represents a special case in that the magnetic moment on Cr2 in the F state is appreciable (1.06 μ_B) whereas it follows the trend for the rest of the series for the AF state (which is 0.20 eV lower in energy than the F state). The *d* electrons in $InCr_3O_8$ may, e.g., be said to participate more in magnetism than in bonding interaction as indicated by the larger Cr2-O bond length in $InCr_3O_8$ (1.68 Å) than that in the other compounds (e.g., 1.63 Å in $TlCr_3O_8$), whereas Cr1-O distance (1.91 Å) is almost equal (1.92 Å in $TlCr_3O_8$). A general feature for the entire ACr_3O_8 family is that the oxygen atoms also possess small magnetic moments which originate from Cr *d* and O *p* hybridization, and this results in somewhat higher total moment values for the F cases than the sum of the Cr moments. The magnetic moments at O atoms range from 0.018 to 0.062 μ_B. The moments at O1 and O3 are directed parallel to the majority-spin channel of Cr atoms while the moments at O2 are directed parallel to the minority-spin channel of Cr atoms. The differ-

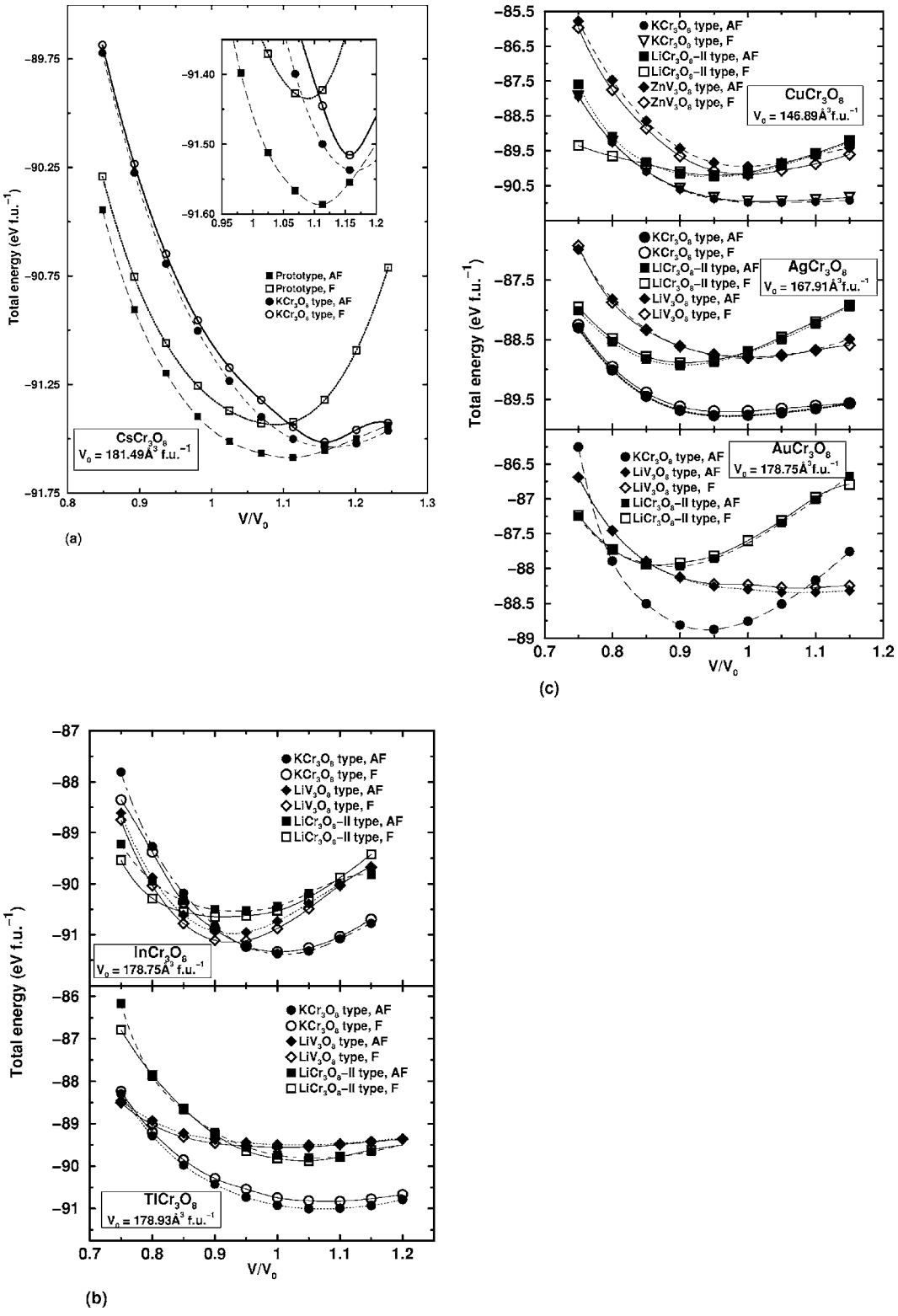

FIG. 2. Calculated cell volume vs total energy for ACr_3O_8 with (a) A=Cs, (b) A=In and Tl, and (c) A=Cu, Ag, and Au.

ent size of the Cr magnetic moments is a clear indication of different valence states. However, our prior experiences[6–8] show that assignment of formal valence states for Cr from their magnetic moments is not straightforward.

C. Electronic structure

All ACr_3O_8 compounds (except $InCr_3O_8$), exhibit insulating behavior at 0 K with small, but distinct band gaps (E_g)

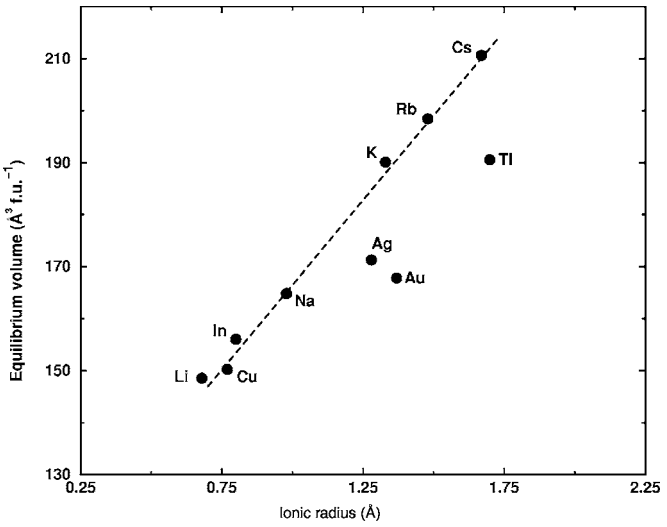

FIG. 3. Optimized equilibrium volume for ACr_3O_8 (A=Li, Na, K, Rb, Cs, In, Tl, Cu, Ag, and Au) as a function of A^+ radius (standard values).

between the valence band (VB) and conduction band (CB). The E_g values for the compounds under consideration are included in Table II. $InCr_3O_8$ has a pseudogaplike feature at the Fermi level (E_F). The presence of pseudogaplike features in DOS is considered as favorable for stability, but this indicator cannot be taken in support of a probable materialization of such a compound. In fact, compounds with monovalent In are relatively uncommon (for instance, only 114 compounds with monovalent In are reported in the ICSD database[18] compared to 1072 compounds with In in the trivalent state) and a standard ionic radius for In^+ is not available. In order to get insight into the occurrence of the higher magnetic moment at the Cr2 site in $InCr_3O_8$ than the other ACr_3O_8 compounds we have examined the total and site-projected DOS for this phase (not shown). Interestingly, this exercise showed a half-metallic behavior with filled band in the majority-spin channel and a 2.6 eV energy gap in the minority-spin channel. The exchange-splitting energy for Cr1 is around 1.5 eV whereas that for Cr2 is 0.8 eV. It is the latter distinct exchange splitting which is responsible for the sizeable magnetic moment at the Cr2 site. It should be noted that owing to the limitation of usual density-functional calculations transition metal oxides are often wrongly predicted to be metal instead of insulator. This can be remedied by going beyond GGA such as LDA+U method,[19] self-interaction corrected density-functional calculations[20] or dynamical mean field theory.[21] Additional calculations with such approaches may clarify why InCr3O8 is metallic rather than insulator. Hence, provided $InCr_3O_8$ can be obtained its properties appear to deserve a closer attention.

Figure 4 shows the total and site-projected DOS profiles for $CsCr_3O_8$ together with $CuCr_3O_8$ as representative for the ACr_3O_8 compounds with KCr_3O_8-type structure. The well-localized states around −7 eV in Fig. 4(a) originate from Cs p orbitals. Cr d and O p states are present from −6 eV up to E_F. The energetic distribution of these DOS profiles show some similarities to those of Cr d and O p DOS in CrO_2 (d^2) and Cr_2O_3 (Ref. 22) which extend from −8 to E_F. Moreover, CrO_2 (Cr in octahedral coordination) and Cr_2O_3 (Cr in square-planar coordination) have Cr-d states closer to E_F like in Cr1 (from −0.9 eV to E_F) which has octahedral coordination. These states are attributed to the unpaired electrons in t_{2g}-like orbitals which are responsible for the substantial magnetic moment at Cr1. Since Cr2 and Cr3 have tetrahedral coordination, their DOS profiles are significantly different from that of the Cr1. The majority- and minority-spin channels of Cr2 and Cr3 are more or less equally filled, resulting in the small magnetic moments. The average Cr1-O distance is 1.94 Å whereas the average Cr2-O and Cr3-O distances are 1.67 Å. This implies that Cr1 states participate more in magnetic interaction than in bonding interaction and vice versa for Cr2 and Cr3. As Cr2 and Cr3 d states participate more in bonding interaction, they are localized and hence no significant states are seen closer to E_F. [It is worthwhile to recall that in a similar compound KCr_3O_8,[6] the integrated crystal orbital Hamiltonian population (COHP) value for tetrahedral Cr is more than the octahedral Cr, implying stronger bonding interaction in the former than in the latter.] It is interesting to note that Cr1, Cr2, Cr3, and O2 states have well-defined sharp peaks around −6 eV. Among the three different types of O, O2 is the one which places itself at the apex of $Cr1O_6$ octahedra and $Cr2O_4$, $Cr3O_4$ tetrahedra. Thus O2 mediates the superexchange interaction between Cr1 and Cr2/Cr3 which is manifested by the DOS peaks seen around −6 eV.

According to our calculations $CuCr_3O_8$ should be a semiconductor with a 0.41 eV band gap. The prominent states for

TABLE II. Calculated magnetic moment (in μ_B per Cr atom) for ACr_3O_8 in F and AF states. Total refers to the total magnetic moment per formula unit. Band gap (E_g) is given in units of eV.

	F			AF		
Compound	Cr1	Cr2	Total	Cr1	Cr2	E_g
$CsCr_3O_8$[a]	2.488	0.231	2.866	2.481	0.233	0.61
$CuCr_3O_8$	2.608	0.231	2.888	2.533	0.018	0.41
$AgCr_3O_8$	2.518	0.249	2.879	2.476	0.000	0.58
$AuCr_3O_8$	2.422	0.226	2.854	2.476	0.011	0.45
$InCr_3O_8$	2.750	1.063	4.776	2.579	0.673	psuedogap
$TlCr_3O_8$	2.495	0.212	2.868	2.422	0.016	0.53

[a]Moment at Cr3 is 0.208 and 0.212 in F and AF states, respectively.

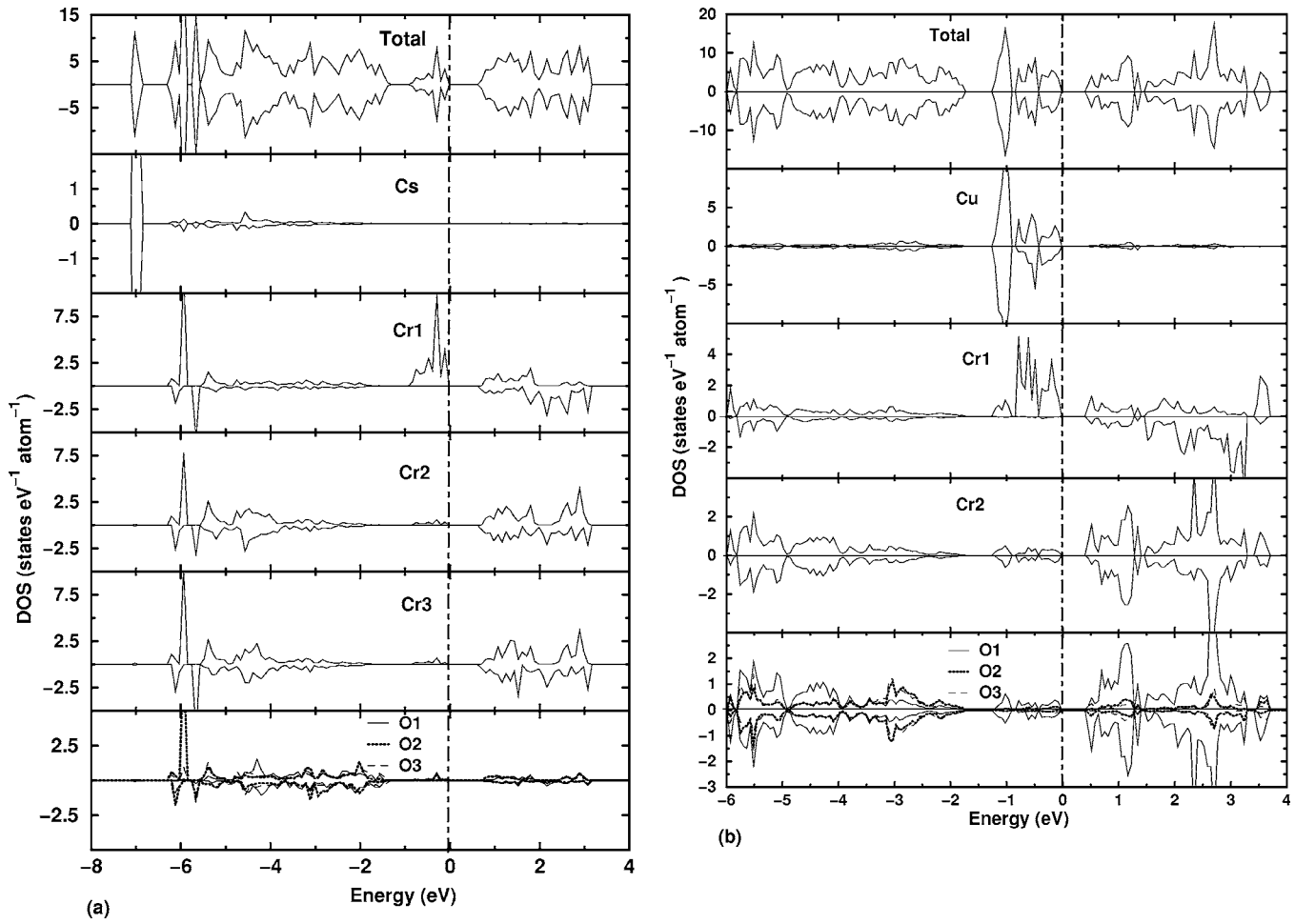

FIG. 4. Total and site-projected density of states for $CsCr_3O_8$ (prototype) and $CuCr_3O_8$ (KCr_3O_8 type). The Fermi level (E_F) is indicated by vertical dashed line.

Cu close to E_F is associated with completely filled d states. The almost empty s and p bands indicate that Cu has donated its valence electron to the oxygen atoms. The two types of Cr atoms have topologically different DOS profiles. The overall features are similar to the findings for the alkali-metal members of the ACr_3O_8 (Refs. 6 and 7) family. Cr1 has sharp peaks close to E_F (from -1.5 to E_F) with more states in the majority-spin channel than in the minority-spin channel. On the other hand, both the majority- and minority-spin channels of Cr2 for $CuCr_3O_8$ are almost equally filled, resulting in negligible exchange splitting and hence in a negligible magnetic moment. From this observation we conclude that small magnetic moment at the Cr2 site is not due to small amount of electrons at the Cr2 state (6+ oxidation state has been expected from simple ionic model). Moreover, the states at the Cr2 site are more localized than those at the Cr1 site [see the -6 to -2 eV range in Fig. 4(b)]. If Cr2 had been in the Cr^{6+} (d^0) state, its d band should have been empty. However, the appreciable DOS seen in the VB of Cr2 demonstrates that the valence state of Cr2 is certainly not Cr^{6+} as expected experimentally. Similar to the findings for the other ACr_3O_8 compounds with KCr_3O_8-type structure, the O atoms exhibit somewhat different DOS profiles, even though they are energetically degenerate with themselves and with the Cr atoms. The result is distinct covalent hybridization.

Mixed-valence compounds have been receiving particular attention as they exhibit interesting optical, electrical and magnetic properties. Most of them are attractive candidates for technological applications owing to their CMR behavior. Even though occurrence of mixed-valence state is common to all transition-metal ions, compounds with Mn have been receiving particular attention, may be due to their potential applications. In order to understand the exotic physical properties exhibited by these interesting compounds, evaluation of the valence states of different ions is imminent. Quite a few empirical rules such as Pauling rules and Hume-Rothery rule are used to ascribe valences for binary and ternary compounds. For compounds with transition-metal species semiempirical Hund's rules are useful to determine spin and valence configurations. The magnetic moment measurements and concepts like bond-valence sums provide qualitative values for valence states. The calculated magnetic moments, site-, and orbital-projected DOS at the transition-metal sites in conjunction with crystal-field effects provide some clues about the valence states. Attempts to derive the formal valences from Born-effective charges for $LiCr_3O_8$ provided 1.36, 3.54, 4.57, and -1.61 for Li, Cr1, Cr2, and O, respectively.[7] One of the reasons for the unexpected valence

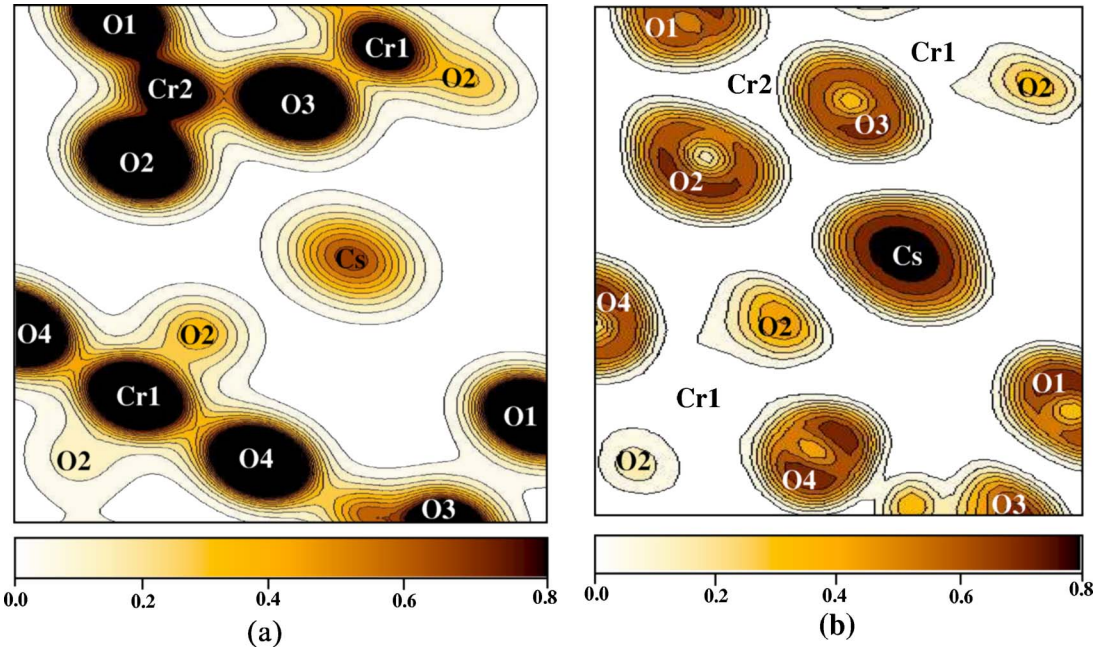

FIG. 5. (Color online) Calculated (a) charge density and (b) electron-localization function for $CsCr_3O_8$.

states of the constituents is that, counting of valence states basically starts from oxygen which is assumed to be ideally in 2- (pure ionic) state. However, in reality valence electrons participate in mixed ionocovalent bonding interactions which result in valence states different from ideally expected values. Since the calculated Born-effective charge values can be considered as upper limits for the formal valence state of a constituent, *A*, Cr1, Cr2, and O can be assigned 1+, 3+, 4+, and 1.5− valence states, respectively.

D. Bonding characteristics

In spite of the fact that the $CsCr_3O_8$ structure possesses 48 atoms in the unit cell which certainly obscures the clarity of the picture, we have attempted to elucidate its bonding characteristics using charge-density and electron localization function (ELF) plots (see Refs. 6–8, 23, and 24 for background information and utilization of these tools for other members of the ACr_3O_8 family). ELF is a measure of the probability of finding an electron near another electron with the same spin. It is a ground state property which discriminates between different kinds of bonding in a very sharp, quantitative way. The ELF is represented as a contour plot in real space where different contour correspond to numerical values ranging from 0 to 1. A region where ELF is 1, there is no chance of finding two electrons with the same spin. This usually occurs in places where bonding pairs (molecular orbitals) or lone pairs (atomic orbitals) reside. An ELF 0 correspond to the area where there is no electron density. For a homogeneous electron gas like in metals ELF is 0.5.[25] It should be noted that ELF is a measure of the Pauli principle and not of electron density. It is seen from Fig. 5(a) that the covalent interaction between Cr2 and O is stronger than that between Cr1 and O. The ionic nature of Cs at the interlayer position is clearly evident from the more or less spherically distributed charge around Cs. The ELF is negligible at the Cr sites whereas it attains local maximum values at the O sites; another manifestation of covalent interaction. The bonding situation in $CsCr_3O_8$ is similar to that seen for other members of ACr_3O_8 family in the sense that chromium and oxygen atoms form ionocovalent-bonded subunits whereas Cs has distinct ionic character. This may be one of the reasons for characteristic magnetic features observed in these compounds.

IV. CONCLUSION

The prediction of ground-state crystal structures for the ACr_3O_8 series have been extended to A=In, Tl, Cu, Ag, and Au considering several potential structure types. The calculated ground-state structure for $CsCr_3O_8$ (space group *Pnma*) is found to be in good agreement with experimental data. Except $NaCr_3O_8$ all members of the ACr_3O_8 family exhibit antiferromagnetic ordering as the ground-state configurations and the electronic structures show that all compounds (except $InCr_3O_8$) are insulators at 0 K; a pseudogaplike feature is established for $InCr_3O_8$. Different magnetic moments and DOS profiles for the Cr atoms clearly confirm mixed-valence situations. Bonding analysis undertaken using density-of-states, charge-density, and electron-localization plots indicate ionic behavior for the *A* atoms whereas the Cr and O atoms mutually experience largely covalent interaction, however, with different degree of covalence for Cr1 and Cr2. In order to have more insight into these compounds, more experimental studies on electrical and magnetic properties are needed.

ACKNOWLEDGMENT

The authors are grateful to the Research Council of Norway for financial support and computer time at the Norwegian supercomputer facilities.

*Electronic address: vidya.ravindran@kjemi.uio.no

[1] C. N. R. Rao and A. K. Raychauduri, in *Colossal Magnetoresistance, Charge Ordering and Related Properties of Manganese Oxides*, edited by C. N. R. Rao and B. Raveau (World Scientific, Singapore, 1998), p. 1.
[2] H. Smolinski, C. Gros, W. Weber, U. Peuchert, G. Roth, M. Weiden, and C. Geibel, Phys. Rev. Lett. **80**, 5164 (1998).
[3] S. G. Bompadre, A. F. Hebard, V. N. Kotov, D. Hall, G. Maris, J. Baas, and T. T. M. Palstra, Phys. Rev. B **61**, R13321 (2000).
[4] R. Melzer and C. H. Ruscher, Phase Transitions **58**, 285 (1996).
[5] J. A. Alonso, M. J. Martínez-Lope, M. T. Casais, J. L. García-Muñoz, and M. T. Fernández-Díaz, Phys. Rev. B **61**, 1756 (2000).
[6] R. Vidya, P. Ravindran, P. Vajeeston, H. Fjellvåg, and A. Kjekshus, Phys. Rev. B **72**, 014411 (2005).
[7] R. Vidya, P. Ravindran, A. Kjekshus, and H. Fjellvåg, Phys. Rev. B (to be published).
[8] R. Vidya, P. Ravindran, A. Kjekshus, and H. Fjellvåg, J. Electroceram. (to be published).
[9] S. Okamoto, S. Ishihara, and S. Maekawa, Phys. Rev. B **63**, 104401 (2001).
[10] P. E. Bløchl, Phys. Rev. B **50**, 17953 (1994); G. Kresse and D. Joubert, *ibid.* **59**, 1758 (1999).
[11] G. Kresse and J. Furthmuller, Comput. Mater. Sci. **6**, 15 (1996).
[12] J. P. Perdew, K. Burke, and Y. Wang, Phys. Rev. B **54**, 16533 (1996); J. P. Perdew, K. Burke, and M. Ernzerhof, Phys. Rev. Lett. **77**, 3865 (1996).
[13] P. Vinet, J. H. Rose, J. Ferrante, and J. R. Smith, J. Phys.: Condens. Matter **1**, 1941 (1989).
[14] K.-A. Wilhelmi, Ark. Kemi **26**, 141 (1966); Chem. Commun. (London) **1966**, 437 (1966); Doctoral thesis, University of Stockholm, Stockholm, 1966.
[15] U. Häussermann, H. Blomqvist, and D. Noréus, Inorg. Chem. **41**, 3684 (2002).
[16] M. J. Saavedra, C. Parada, and E. J. Baran, J. Phys. Chem. Solids **57**, 1929 (1996).
[17] H. Fjellvåg (unpublished).
[18] Inorganic Crystal Structure Database, Version 2004.2.
[19] A. I. Liechtenstein, V. I. Anisimov, and J. Zaanen, Phys. Rev. B **52**, R5467 (1995).
[20] A. Svane and O. Gunnarsson, Phys. Rev. Lett. **65**, 1148 (1990).
[21] A. Georges, G. Kotliar, W. Krauth, and M. Rozenberg, Rev. Mod. Phys. **68**, 13 (1996).
[22] R. Zimmermann, P. Steiner, R. Claessen, F. Reinert, S. Hüfner, P. Blaha, and P. Dufek, J. Phys.: Condens. Matter **11**, 1657 (1999).
[23] P. Ravindran, P. Vajeeston, R. Vidya, A. Kjekshus, and H. Fjellvåg, Phys. Rev. Lett. **89**, 106403 (2002).
[24] A. Savin, R. Nesper, S. Wengert, and T. Fässler, Angew. Chem., Int. Ed. Engl. **36**, 1809 (1997).
[25] N. Oai and J. B. Adams, J. Comput. Electron. **3**, 51 (2004).